

# Bio-Nanohybrid Composite Sorbent-Based Microextraction Combined with High-Performance Liquid Chromatography for NSAIDs in Aqueous Samples

Nor Suhaila Mohamad Hanapi<sup>1</sup>, Nur Husna Zainal Abidin<sup>1</sup>, Wan Nazihah Wan Ibrahim<sup>1\*</sup>,  
Nordiana Suhada Mohamad Tahiruddin<sup>2</sup>, Nurul Auni Zainal Abidin<sup>3</sup>,  
Roswanira Abdul Wahab<sup>4</sup> and Sheela Chandren<sup>4</sup>

<sup>1</sup> Faculty of Applied Sciences, Universiti Teknologi MARA, 40450 Shah Alam, Selangor, Malaysia

<sup>2</sup> Faculty of Applied Sciences, Universiti Teknologi MARA, Perak Branch, 35400 Tapah, Perak, Malaysia

<sup>3</sup> Faculty of Applied Sciences, Universiti Teknologi MARA, Negeri Sembilan Branch,  
72000 Kuala Pilah, Negeri Sembilan, Malaysia

<sup>4</sup> Department of Chemistry, Faculty of Science, Universiti Teknologi Malaysia,  
81310 Johor Bahru, Johor Malaysia.

\*Corresponding author (e-mail: wannazihah@uitm.edu.my)

Chitosan was hybridised with tetraethoxysilane via hydrolysis to obtain a bio-nanohybrid composite sorbent for dispersive solid-phase extraction (DSPE) of three non-steroidal anti-inflammatory drugs in aqueous samples. Field Emission Scanning Electron Microscope (FESEM) micrographs showed that the bio-nanohybrid composite was composed of spherical-shaped nanoscale particles with sizes ranging from 41.1 - 231.5 nm. The effects of three significant parameters, namely extraction time, sample pH, and desorption time, on the determination of naproxen (NAP), diclofenac sodium (DIC), and mefenamic acid (MEF), were evaluated systematically using the Box Behnken design (BBD).  $R^2$  was found to be 0.942 for NAP, 0.966 for DIC and 0.960 for MEF. These results were all close to 1.0, indicating good correlation between predicted and observed values. Under optimized conditions, the DSPE showed good linearity over the range of 0.1 - 500  $\mu\text{gL}^{-1}$ , low detection limits (0.04-0.67  $\mu\text{g/L}$ ), excellent limits of quantification (0.15-2.78  $\mu\text{gL}^{-1}$ ), excellent relative recoveries (93.06-101.48%) and acceptable precision with relative standard deviation (RSD) values < 7.75%. These results indicate that this bio-nanohybrid composite is a promising sorbent for sorbent-based microextraction and a good alternative to synthetic polymer sorbents.

**Key words:** Chitosan; nanohybrid; dispersive solid phase extraction; Box Behnken design; non-steroidal anti-inflammatory

*Received: December 2021; Accepted: February 2022*

Natural biodegradable polymers such as polysaccharides can be extracted from marine plants and animals. They are naturally abundant and rich in native functional groups that can be tailored to sorption requirements. The extraction efficiency of the sorption process is influenced by functional groups present in the sorbent material. Variation in functional groups contributes to an increase in active sites that allow interactions with analytes and enhance adsorption activity. Chitosan is extracted from the exoskeleton of marine organisms with large amounts of primary amino (-NH<sub>2</sub>) and hydroxyl (-OH) groups in their backbone polymer matrix. The presence of these groups allow chemical and electrostatic interactions, thus creating possibilities for chemical modification [1,2]. Theoretically, these native functional groups could turn chitosan into a promising biopolymer-based sorbent with an excellent capacity to entrap trace level residues [3]. However, it is quite challenging to directly use this biomass in the form of

flakes or powder in wastewater treatment due to its disadvantages such as swelling, unsatisfying mechanical properties, and mass transfer resistance. Chitosan suffers from pH sensitivity because the amino groups in the chitosan backbone are easily protonated and completely soluble under acidic conditions [1,4-5]. Chitosan partially dissolves at pH 3.0 and instantaneously dissolves at pH 1.2 [6].

A practical way to circumvent these problems is to hybridize chitosan with other materials such as porous silica nanoparticles to form bio-hybrid composite materials. Porous silica has excellent physicochemical properties such as high surface area, high pore volume, chemical inertness, good thermal stability, excellent mechanical resistance, and low manufacturing cost. This material is rich in a number of surface functional groups with excellent selectivity towards specific pollutants [7]. Thus, by hybridizing silica nanoparticles with a high-density biopolymer,

the resulting chitosan matrix would be an effective alternative to improve the sorbent's mechanical strength and increase mass density [8-10].

In this work, a bio-nanohybrid chitosan-tetraethoxysilane (Ch-TEOS) composite was prepared as a composite sorbent to determine selected non-steroidal anti-inflammatory drugs (NSAIDs). The selected drugs, naproxen (NAP), diclofenac sodium salt (DIC), and mefenamic acid (MEF), were chosen as models based on the most consumed pharmaceuticals frequently used for suppressing inflammatory processes. These drugs were analyzed via a dispersive solid-phase extraction (DSPE) prior to high-performance liquid chromatography/Ultraviolet-Visible detector (HPLC/UV) analysis. This study used Response surface methodology (RSM) with the Box-Behnken Design (BBD) to improve the DSPE performance, focusing on factors *viz.* extraction time, sample pH, and desorption time for the determination of NAP, DIC, and MEF. Optimization was necessary to minimize the use of resources and better evaluate the interactions of variables that profoundly affected the DSPE method. Therefore, this study aimed to enrich the body of knowledge on nanohybrid biocomposites for potential use in DSPE for drug analysis.

## MATERIALS AND METHODS

### Reagents, Materials and Samples

NSAID standards were purchased from Sigma-Aldrich (St. Louis, USA). HPLC-grade organic solvents acetonitrile (ACN), methanol (MeOH), ethanol (EtOH), and isopropanol (IPA) were obtained from J.T. Baker (USA) and Merck (Germany). Reagent grade sodium chloride (NaCl) was purchased from Bendosen (Malaysia). Sodium hydroxide 99% (NaOH) and hydrochloric acid 97% (HCl) were obtained from Merck (Germany). Acetic acid glacial 100% was purchased from Qrec (New Zealand). Ammonium hydroxide, chitosan, and tetraethoxysilane (TEOS) were obtained from Sigma-Aldrich (USA). Deionized water of at least 18 mΩ was obtained from a Nano ultra-pure water system (USA). The standard solutions were prepared by dissolving in HPLC grade MeOH, and were stored in the dark at 4°C when not in use. The water samples were collected in bottles pre-cleaned with acetone, filtered through a nylon membrane filter to remove colloidal particles, and stored in a refrigerator at 4°C for further use.

### Instrumentation

A HPLC/UV system was used, consisting of a JASCO PU-980 pump (Japan) and a Shimadzu UV-Visible detector (Japan). A Rheodyne 7725 valve with a 20 µL sample loop (USA) was used for sample introduction. Separations were performed on an Agilent Technology Zorbax Eclipse Plus C<sub>18</sub> column (3.5 µm, 100 mm length × 2.1 mm I.D.) (USA). A 2 µL sample

was injected using a Hamilton HPLC syringe (USA). The measured ultraviolet wavelength was 230 nm, as in previous reports [11-12], and the analyte peaks were recorded using a Powerchrom data recording system (eDAQ, Australia). The mobile phase consisted of acetonitrile-acetate buffer (pH 3.2, 25 mM) (50:50, v/v), and the flow rate was 0.2 mL/min in isocratic mode. Each sample was filtered through a 0.45 µm syringe filter (Membrane Solution Nylon) before injection.

The extraction procedure involved using a Heidolph Reax 2000 vortex agitator (Germany) to assist the extraction process and a Branson CPX ultrasonic bath (USA) to assist the desorption of analytes from the composite sorbent.

Characterization of the Ch-TEOS bionanohybrid composite sorbent was performed using a Perkin Elmer Frontier Attenuated Total Reflection Fourier Transform Infrared (ATR-FTIR) spectrophotometer (USA) in the range of 4000 - 650 cm<sup>-1</sup> with a resolution of 4 cm<sup>-1</sup> averaging 24 scans. The morphology study of the composite was performed on a JEOL JSM-7600F Ultra High-Resolution Field Emission Scanning Electron Microscope (FESEM) with a magnification of 1000X to 25000X, while the Brunauer-Emmett-Teller (BET) pore analysis used the Micromeritics 3Flex Surface Characterization Analyzer (USA).

### Preparation of Bio-Nanohybrid Composite Sorbent

The Ch-TEOS bio-nanohybrid composite was synthesized via a hydrolysis technique with some modifications [13]. Silica solution was prepared by mixing 5 mL of tetraethoxysilane with 15 mL of ethanol, 1 mL of deionized water and 0.5 mL of concentrated hydrochloric acid (37%). The mixture was stirred using a magnetic stirrer for 10 min. This solution was slowly added to the previously prepared chitosan solution (0.25 g of chitosan dissolved in 50 mL of 2% acetic acid) and continuously stirred for 24 h. The combined solution was then added dropwise into concentrated ammonium (38%) to form a white, cloudy solution, and this mixture was stirred for 2 h. The white solid product was separated using 11 µm filter paper, rinsed thoroughly with deionized water, and dried in the oven at 50 °C for 24 h.

### Dispersive Solid-Phase Extraction (DSPE)

50 mg of Ch-TEOS bio-nanohybrid composite sorbent was added into a 50-mL centrifuge tube containing 10 mL of the aqueous sample at pH 4.13. The sample was vortexed for 14.05 min at 450 rpm. The sorbent was then separated from the solution by centrifugation at a speed of 4000 rpm for 5 min, and the supernatant was discarded. The desorption of analytes was performed with 300 µL of ACN under ultrasonication for 5 min, and the solution was filtered through a 0.45µm

polypropylene syringe filter. The solution was then pre-concentrated to 100  $\mu$ L under a gentle stream of nitrogen gas for analyte enrichment. A 2  $\mu$ L aliquot of the final extract was analyzed by HPLC/UV at 230 nm. Figure 1 shows the schematics of this method, termed as Ch-TEOS-DSPE-HPLC/UV.

### Experimental Design and Statistical Analysis

We have previously developed analytical methods for similar drugs and identified the five most significant parameters [14]. Thus, preliminary experiments were carried out using a classical approach by varying one-variable-at-a-time (OVAT) to identify the significant parameters that affected the adsorption process due to the different types of sorbents and techniques applied. In this study, the parameters assessed were: the addition of salt, sample pH, extraction time, type of desorption solvent, and desorption time. In the BBD optimization experiment, the study only selected three significant parameters from the OVAT study. For the BBD, Design-Expert software version 13 (Stat Ease Software, USA) was used to optimize the DSPE process for: extraction time (A), pH of sample (B), and desorption time (C), for the response

extraction efficiency (mV.s) of NAP, DIC and MEF. The ranges and coded levels of the BBD variables are listed in Table 1. The lower, central and upper ranges and levels were obtained from previous OVAT studies. In this study, the quality of fit of the generated polynomial model equation was gauged using the coefficient of determination ( $R^2$ ), and the responses were analyzed using analysis of variance (ANOVA). A p value < 0.05 indicates a significant model term. Other main indicators to illustrate the significance and adequacy of the generated model include the model's lack of fit, F-value and signal-to-noise ratio.

### Validation of Analytical Method

The DSPE method was assessed for linearity ( $R^2$ ), limits of detection (LOD), limits of quantification (LOQ), precision and accuracy to ensure that the analytical procedure was reliable and fit for the intended purpose. LOD and LOQ values were calculated based on linear regression of the calibration curve. Precision was expressed in terms of relative standard deviation (RSD %) and accuracy (% relative recovery).

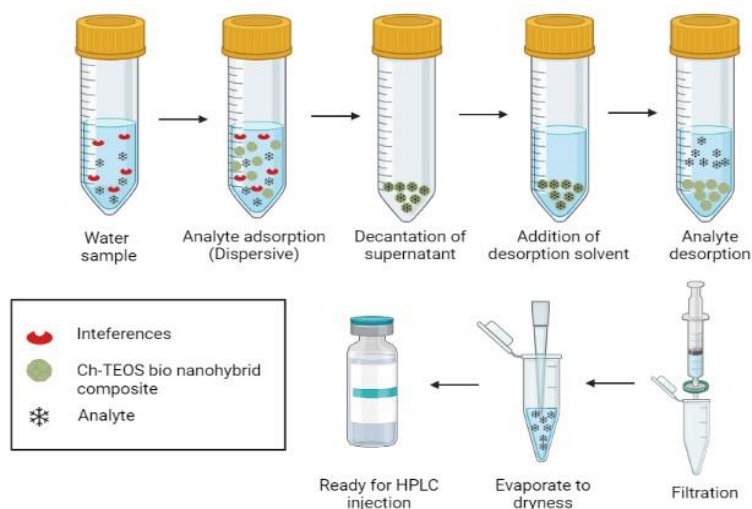


**Figure 1.** Schematic diagram of the method termed as Ch-TEOS-DSPE-HPLC/UV

**Table 1.** The BBD independent variables and their levels in the DSPE optimization experiment

Variable	Unit	Key	Type	Range and levels		
				Lower	Central	Upper
Extraction time	min	A	Numeric	5	10	15
pH of sample	pH	B	Numeric	2	4	6
Desorption time	min	C	Numeric	5	10	15

## RESULTS AND DISCUSSION

### Characterization of Bio-Nanohybrid Ch-TEOS Composite Sorbent

The Ch-TEOS bio-nanohybrid composite was obtained as a white powder in non-crystalline form. Table 2 summarizes the significant adsorption bands of functional groups present in pristine chitosan, TEOS, and the Ch-TEOS bio-nanohybrid composite. The broad absorption band of hydroxyl (O-H) stretching vibrations appeared notably weaker and shifted from  $3649\text{ cm}^{-1}$  in pristine chitosan to  $3607\text{ cm}^{-1}$  in Ch-TEOS, indicating that the H atom in O-H had been partly grafted to the silica group [15]. The amino groups ( $-\text{NH}_2$ ) of chitosan, as expected, facilitate the hydrolysis of the silanolate (Si-OR) groups to form a linkage with the polymer chain of chitosan. Thus, the absorption band at  $1686\text{ cm}^{-1}$  corresponds to vibrations of amino groups in chitosan that shifted to  $1678\text{ cm}^{-1}$  in Ch-TEOS, suggesting weak interactions between the amino groups and the silica network. An intense absorbance at  $1072\text{ cm}^{-1}$  represents the Si-O stretching vibration in TEOS that deformed into a wide band at  $1065\text{ cm}^{-1}$  in Ch-TEOS, confirming the covalent Si-O-C bonds in the hybrid composite [13].

FESEM analysis of the Ch-TEOS hybrid composite was essential to determine the surface interactions of TEOS and the homogeneity of the chitosan matrix. The surface morphology of the granule form, pristine chitosan, resembled dense fibres [16-17]. However, the micrograph of Ch-TEOS at high magnification (25000X) (Figure 2) revealed spherical-shaped particles in the bio-nanohybrid composite. The structure seen here

confirmed that the inorganic silica moiety was trapped and condensed into the chitosan network which led to the observed morphological change. Likewise, similar observations were reported by earlier studies [18-19]. Pertinently, the FESEM measurements revealed that the bio-nanohybrid composite had particles of 41.1-231.5 nm, verifying the presence of nanoparticles in the sorbent.

Data from the Brunauer-Emmett-Teller (BET) and nitrogen adsorption analysis showed that introducing large-structured TEOS into pristine chitosan profoundly influenced the surface properties of the resultant composite. The surface area of Ch-TEOS increased to  $148.94\text{ m}^2\text{g}^{-1}$  compared to  $3.27\text{ m}^2\text{g}^{-1}$  for pristine chitosan [15]. The average pore diameter was  $92.99\text{ \AA}$ , with a corresponding total pore area of  $56.05\text{ m}^2\text{g}^{-1}$ . The data thus indicated that high surface area mesoporous structures existed in the bio-nanohybrid composite [13, 20]. It should be pointed out that particles with a large surface area are better choices for sorbent materials, allowing more active sites for adsorption.

### Optimization of the Ch-TEOS-DSPE -HPLC/UV Method

Based on a similar drug analysis in previous studies [21-24], five parameters that significantly affected the microextraction process were identified. A preliminary study using the classical approach by OVAT was undertaken to investigate the effect of salt addition and desorption time. The presence of salt in water samples can disrupt the solvation cage of the water-soluble analytes (salting-out effect) and alter the diffusion rate of analytes toward the sorbent surface.

**Table 2.** Comparison of FTIR absorption bands in Chitosan, TEOS, and the Ch-TEOS bio-nanohybrid composite

Vibration	Chitosan ( $\text{cm}^{-1}$ )	TEOS ( $\text{cm}^{-1}$ )	Ch-TEOS ( $\text{cm}^{-1}$ )
O-H stretching	3649	-	3607
N-H bending	1686	-	1678
Si-O stretching	-	1072	1065

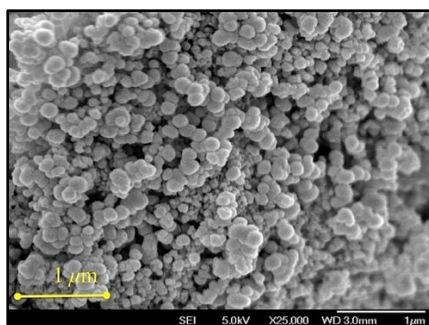


**Figure 2.** FESEM images of the Ch-TEOS bio-nanohybrid composite

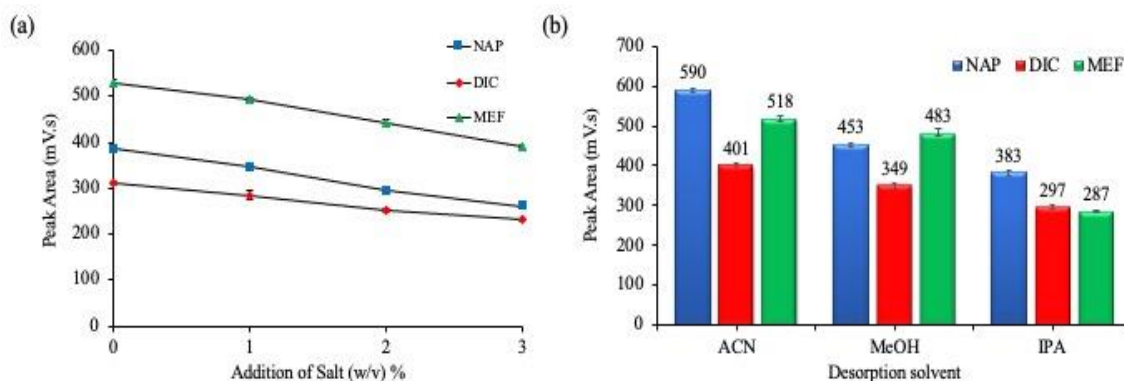


**Figure 3.** (a) Effect of salt addition; (b) Effect of desorption solvent

In this study 0 - 3 % (w/v) of salt was added, but the extraction efficiency was not improved (Figure 3 (a)). In a prior investigation, a similar phenomenon of diminishing extraction efficiency after the addition of salts was noted, as the salt counter ion in the sample solution had outcompeted the target analytes [25]. Consequently, the subsequent experiments were done in the absence of salt.

The study was then performed on the desorption of extracted analytes from the sorbent using three HPLC-compatible organic solvents of different polarity indices, namely acetonitrile (5.8), methanol (5.1) and isopropanol (3.9). Figure 3(b) showed that the highest extraction performance based on measured peak area was obtained for the relatively polar acetonitrile, followed by methanol and isopropanol. The outcome correlated well with the relatively polar NSAIDs, in which polar desorption solvents could better desorb these acidic substances compared to less polar solvents [26]. Hence, based on this finding, the subsequent desorption experiment utilized acetonitrile as the solvent.

In the next part of the study, three independent parameters, namely extraction time (A), pH of sample (B), and desorption time (C), were optimized by the BBD approach for the simultaneous microextraction of Ch-TEOS-HPLC-UV using Design-Expert version 13 software. This design produced a total of 16 experiments in which each extracted water sample was spiked with 100  $\mu\text{g L}^{-1}$  NAP, and 500  $\mu\text{g L}^{-1}$  DIC and MEF, respectively. The  $R^2$  value is presented to determine whether there was a good relationship between the predicted and actual values. As shown in Table 3,  $R^2$  was found to be 0.942 for NAP, 0.966 for DIC and 0.960 for MEF. All values were close to 1.0, which indicates a high correlation between predicted and observed values. A very high  $R^2$  value implies excellent correlation and a satisfactory model for predicting the best conditions for the highest extraction efficiency. The model is considered a good fit if the value of the coefficient of determination,

$R^2$  is  $\geq 0.80$  [27].

ANOVA analysis of the BBD showed relatively high F values of 12.70, 22.24, and 18.85 for NAP, DIC, and MEF, respectively (Table 3), indicating the variation between the data was sufficient to be used for model construction. The experimental data also closely agreed with the predicted values, as they were scattered closely along the trend line (Figure 4). Also, the F-values of the model, 12.7, 22.24 and 18.85 for NAP, DIC and MEF, respectively, were greater than the tabulated  $F_{0.05}(9,7) = 3.6767$ , indicating a highly significant degree of freedom relative to the residual at the 95% confidence level.

Finally, the model's lack-of-fit F-values of 0.64 for NAP, 2.31 for DIC and 1.34 for MEF respectively, were considerably lower than the tabulated  $F_{0.05}(3,4) = 6.5914$ , indicating that the lack of fit was insignificant relative to the pure error (Table 3). As for 'adequate precision', this was measured by the signal to noise ratio. A ratio greater than 4 is desirable. Thus, the relatively high ratios of 11.120 (NAP), 18.246 (DIC) and 13.819 (MEF) indicated adequate signals for the model. Therefore, these models could be used to navigate the design space.

For the DSPE systems, ANOVA indicated that the linear terms A (extraction time) and B (pH of the sample) were significant ( $p$  value  $< 0.05$ ), but not C (desorption time). Only the mutually interactive term, AC (extraction time versus desorption time) was significant, with  $p$  values of 0.0005 for NAP, 0.001 for DIC and 0.005 for MEF, while the interactions of extraction time versus pH of sample (AB) and pH of sample versus desorption time (BC) were borderline insignificant. As the constructed plots exhibited the presence of a saddle point, the study resorted to using ridge maximum and canonical analyses to establish the critical levels of the design variables which maximized the extraction efficiencies of the NSAIDs.

**Table 3.** ANOVA of the response surface quadratic model for three selected NSAID analytes

<i>Analyte</i>	<i>Source</i>	<i>Sum of Squares</i>	<i>DF</i>	<i>Mean Square</i>	<i>F Value</i>	<i>p-value</i>		
NAP	Model	147900	9	16437	12.7	0.0015	significant	
	A	1516	1	1516	1.17	0.3151		
	B	70519	1	70519	54.47	0.0002		
	C	704	1	704	0.54	0.4848		
	A2	18719	1	18719	14.46	0.0067		
	B2	2125	1	2125	1.64	0.2409		
	C2	646	1	646	0.5	0.5029		
	AB	3628	1	3628	2.8	0.138		
	AC	48949	1	48949	37.81	0.0005		
	BC	819	1	819	0.63	0.4526		
	Residual	9062	7	1295				
	Lack of Fit	2948	3	983	0.64	0.6266		not significant
	Pure Error	6114	4	1529				
	Cor Total	157000	16					
R <sup>2</sup>	0.942			Adeq. Precision	11.120			
DIC	Model	106900	9	11873	22.24	0.0002	significant	
	A	28483	1	28483	53.35	0.0002		
	B	44206	1	44206	82.8	< 0.0001		
	C	371	1	371	0.7	0.4319		
	A2	9460	1	9460	17.72	0.004		
	B2	1137	1	1137	2.13	0.1878		
	C2	3901	1	3901	7.31	0.0305		
	AB	705	1	705	1.32	0.2882		
	AC	15738	1	15738	29.48	0.001		
	BC	2697	1	2697	5.05	0.0594		
	Residual	3737	7	534				
	Lack of Fit	2370	3	790	2.31	0.2179		not significant
	Pure Error	1367	4	342				
	Cor Total	110600	16					
R <sup>2</sup>	0.966			Adeq. Precision	18.246			
MEF	Model	598900	9	66544	18.85	0.0004	significant	
	A	18832	1	18832	5.33	0.0542		
	B	34975	1	34975	9.91	0.0162		
	C	7619	1	7619	2.16	0.1853		
	A2	13998	1	13998	3.97	0.0867		
	B2	371600	1	371600	105.26	< 0.0001		
	C2	1492	1	1492	0.42	0.5364		
	AB	2552	1	2552	0.72	0.4234		
	AC	133500	1	133500	37.82	0.0005		
	BC	787	1	787	0.22	0.6512		
	Residual	24713	7	3530				
	Lack of Fit	12382	3	4127	1.34	0.3799		not significant
	Pure Error	12331	4	3083				
	Cor Total	623600	16					
R <sup>2</sup>	0.960			Adeq. Precision	13.819			

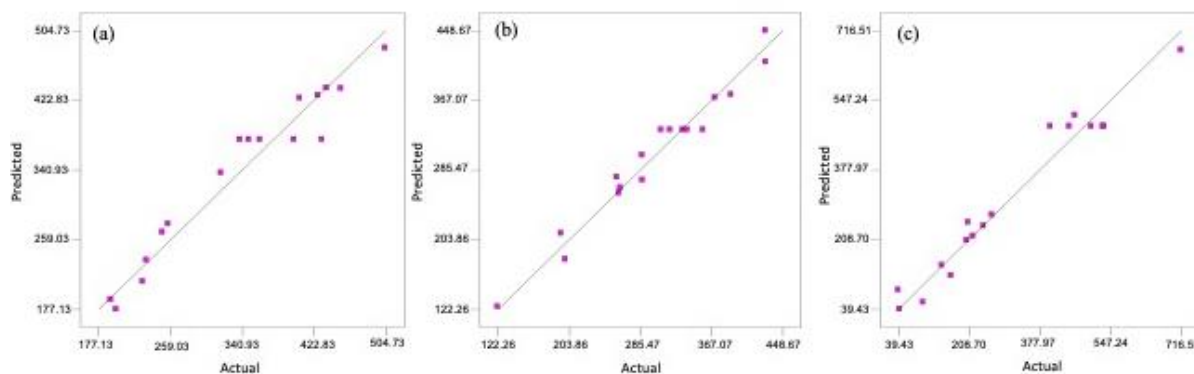


**Figure 4.** Relationship between predicted vs actual values for (a) NAP, (b) DIC and (c) MEF

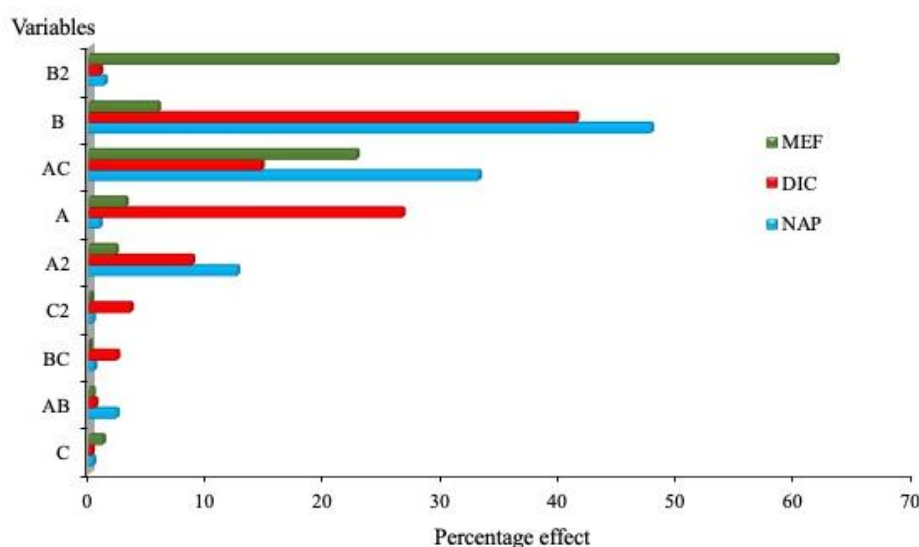


**Figure 5.** Pareto chart of percentage effects of parameters of single factors, squared factors and interaction factors for the optimization of Ch-TEOS-DSP-HPLC/UV analysis of NSAIDs.

A: Extraction time, B: pH of sample, C: desorption time

A comparison of single factors (Figure 5) showed that the sample pH, B, had the most impact on the extraction efficiencies for all NSAIDs at 1.4-63.5%, followed by extraction time, A (1.0-26.7%), and finally desorption time, C (0.3-1.3%). This behaviour was expected because previous studies have shown that the sample pH influences the ionization of analytes, allowing their effective adsorption onto the adsorbent. Furthermore, the low pKa values of NSAIDs cause them to adopt a predominantly neutral form at low pH and become protonated at relatively higher pH [11].

In this work, the hyperbolic contour plots for NAP and DIC extraction efficiencies (Figure 6(a) and (b)) indicate a slight interaction between extraction time and sample pH. Higher extraction times and lower pH values yielded the highest extraction efficiencies. However, extraction time affected the outcome more than pH, which is

consistent with a previous report that showed how extraction time had an appreciable role in controlling mass transfer between phases [28]. Although extraction efficiency tends to increase with prolonged extraction time, extending the extraction time is not always practical. An appropriate length of time must be chosen to maximize the merits of the microextraction technique. In contrast, the half-cylindrical contour plot of MEF (Figure 6 (c)) implied that only pH significantly ( $p$  value  $< 0.05$ ) affected the extraction efficiency. The variation in sample pH results in the variation of surface charge, thus affecting the adsorption efficiencies of the analytes on the sorbent. From this study, it was found that a better absorption of NSAIDs by the sorbent could be achieved at pH 4, which is probably due to the surface of Ch-TEOS being protonated under acidic conditions, allowing for electronic interactions while maintaining hydrophobic interactions towards analytes. [29].

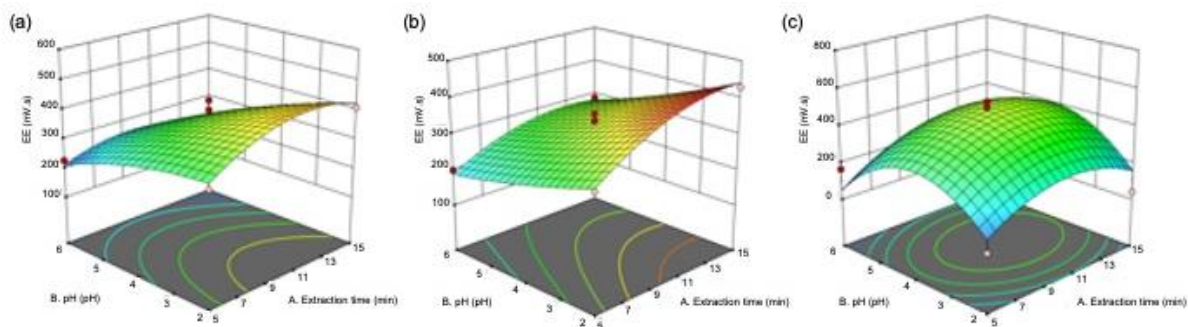


**Figure 6.** Response surface and contour plots of the effect of pH and extraction time on the Ch-TEOS-DSPE-HPLC/UV extraction efficiency (EE) for (a) NAP, (b) DIC, and (c) MEF

Figure 7 shows contour plots of the interactions between (C) desorption time versus (B) pH of the sample for the three analytes. The slanting planar contour plots for NAP and DIC extraction efficiencies showed slight interactions between factors. Meanwhile, the effect of desorption time (F value = 0.7) was appreciably less dominant than sample pH (F value = 82.8), based on the larger F value of the latter. The peak areas of NAP and DIC significantly increased with desorption time and decreased with the increase in sample pH, which suggests that, in the latter, the optimal threshold of the two parameters has been exceeded. Conversely, the half-cylindrical plot of MEF extraction efficiency showed that only sample pH influenced extraction efficiency.

For the comparison of interaction factors (Figure 5), the highest effect on overall extraction efficiency (12.7%) occurred when extraction time (A) mutually interacted with desorption time (C).

Meanwhile, the interactions between sample pH (B) and extraction time (A) or desorption time (C) only mildly affected the extraction efficiency of NSAIDs (up to 2.5%). Figure 8 illustrates the curved planar-shaped plot for the mutual interaction between extraction time (A) and desorption time (C), being crucial to maximizing the NSAIDs extraction efficiency. The extraction efficiency increased proportionally with increasing extraction time (A) and decreasing desorption time (C). It slightly declined for extraction times of > 13 min, which correlates well with their significant interaction as shown in the ANOVA table (p value 0.001) (Table 3). The extended extraction time had likely elevated the system's temperature during the ultrasonication desorption and partially degraded some analytes [21]. From the ANOVA table and contour plot obtained from this study, the order in which the three tested parameters affected the extraction efficiency of NSAIDs is as follows: pH of sample > extraction time > desorption time.

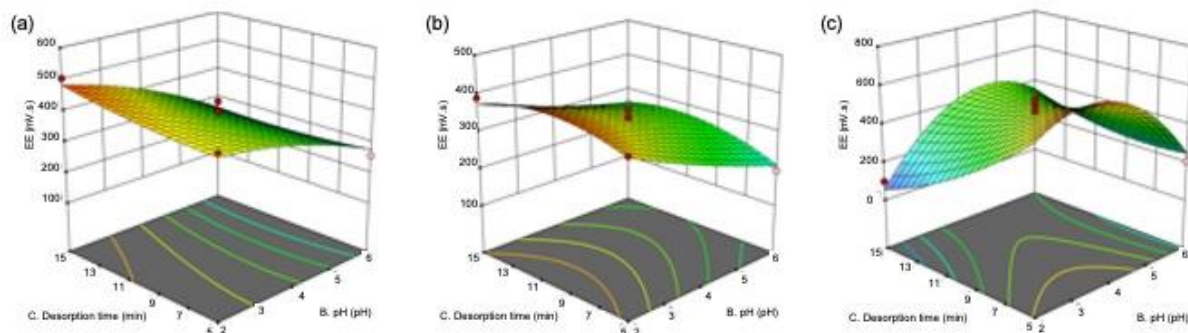


**Figure 7.** Response surface and contour plots of the effect of pH and desorption time on the Ch-TEOS-DSPE-HPLC/UV extraction efficiency (EE) for (a) NAP, (b) DIC, and (c) MEF

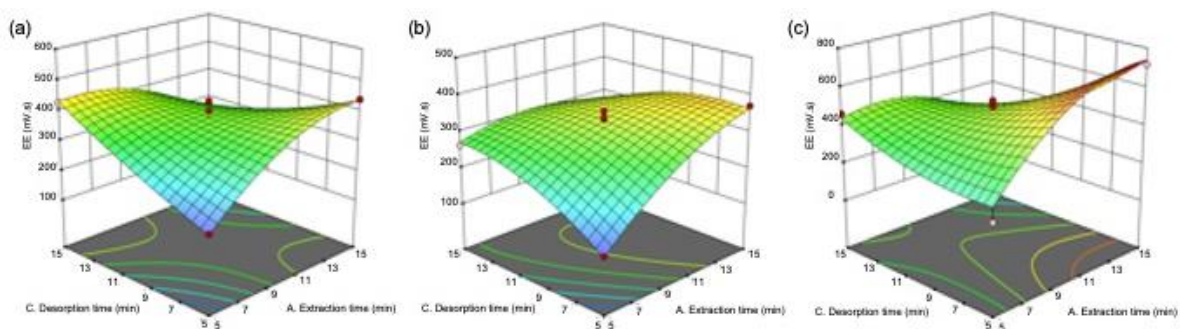


**Figure 8.** Response surface and contour plots of the effect of extraction time and desorption time on the Ch-TEOS-DSPE-HPLC/UV extraction efficiency (EE) for (a) NAP, (b) DIC and (c) MEF

**Validation of Ch-TEOS-DSPE-HPLC/UV Method**

The DSPE optimization experiment was validated to check for the generated model’s reliability to establish the best conditions. Based on the BBD study, the optimum conditions for Ch-TEOS-DSPE-HPLC/UV were 14.05 min extraction time at pH

4.13 with a 5 min desorption time, while holding other variables constant (0.05 g sorbent loading, vortex speed at 450 rpm, and 100  $\mu$ L acetonitrile as desorption solvent). The chromatogram revealed that all analytes were successfully extracted and separated from both water samples with retention times < 13 min (Figure 9).

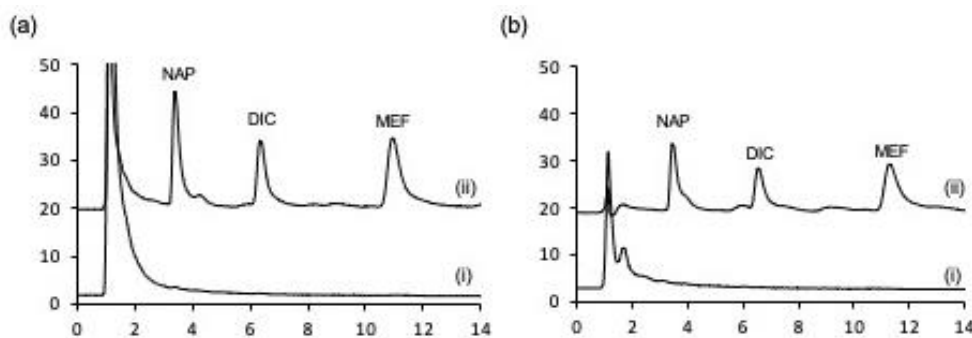


**Figure 9.** Chromatograms of (i) blank and (ii) spiked analytes in (a) tap water and (b) lake water under optimal conditions.

**Table 4.** Validation of Ch-TEOS-DSPE-HPLC/UV method

Samples	Analyte	Linearity range ( $\mu\text{gL}^{-1}$ )	$r^2$	LOD ( $\mu\text{gL}^{-1}$ )	LOQ ( $\mu\text{gL}^{-1}$ )	Spike concentration ( $\mu\text{gL}^{-1}$ )	Average relative recovery %	RSD %
Tap water	NAP	0.1-100	0.998	0.04	0.15	1	97.94	2.82
						80	97.24	4.86
	DIC	1-500	0.999	0.52	2.07	10	98.10	2.27
Lake water	NAP	0.1-100	0.999	0.05	0.20	1	93.06	7.75
						80	101.48	3.35
	DIC	1-500	0.998	0.67	2.78	10	97.24	7.47
MEF	1-500	0.998	0.41	1.62	10	96.16	5.65	
					400	101.40	2.42	
MEF	NAP	0.1-100	0.999	0.05	0.20	1	93.06	7.75
						80	101.48	3.35
	DIC	1-500	0.998	0.67	2.78	10	97.24	7.47
MEF	1-500	0.998	0.59	2.44	10	94.05	5.61	
					400	97.66	2.27	

**Table 5.** Comparison of the Ch-TEOS- DSPE-HPLC/UV method with other published methods for the analysis of NSAIDs in aqueous samples

<i>Method</i>	<i>Instrument</i>	<i>Type of sorbent</i>	<i>Sorbent amount (mg)</i>	<i>LOD (<math>\mu\text{gL}^{-1}</math>)</i>	<i>Extraction time (min)</i>	<i>Ref.</i>
SPE	LC/MS	MCM-41	100.0	0.10 - 3.85	-	[30]
MA- $\mu$ -SPE	HPLC/DAD	UPS	20.0	0.48 - 1.79	60	[31]
MSPE	HPLC/UV	Fe <sub>3</sub> O <sub>4</sub> -polypyrrole	20.0	0.9 – 3.5	2.4	[11]
DSPE	HPLC/UV	Ch-TEOS	50.0	0.04 – 0.67	14	This work

Abbreviations: SPE = solid phase extraction, MA- $\mu$ -SPE = membrane assisted micro-solid phase extraction, DSPE = dispersive solid phase extraction, MCM-41 = mesoporous material 41, UPS = ureidopropyl-grafted silica gel, Ch-TEOS = chitosan-tetraethoxysilane hybrid composite.

The plotted calibration curves based on peak area response vs analyte concentration were also linear ( $r^2 \geq 0.998$ ), ranging between 0.1-100  $\mu\text{g L}^{-1}$  (NAP) and 1–500  $\mu\text{g L}^{-1}$  (DIC and MEF) (Table 4). The limit of detection (calculated based on a signal-to-noise ratio of 3:1) ranged between 0.04-0.67  $\mu\text{gL}^{-1}$  and yielded excellent LOQs (0.15-2.78  $\mu\text{gL}^{-1}$ ). The subsequent recovery study performed using spiked water samples ( $n = 3$ ) gave final concentrations of 1 and 80  $\mu\text{gL}^{-1}$  for NAP, and 10 and 400  $\mu\text{gL}^{-1}$  for DIC and MEF. Excellent recovery values of 93.06 to 101.48% were obtained at an acceptable reproducibility (relative standard deviation of  $< 7.75\%$ ). The results revealed that this method could be applied in therapeutic drug monitoring and environmental water analysis.

Table 5 summarizes the comparisons between the chromatographic method, types of silica-based sorbent used, and LODs to determine NSAIDs in aqueous samples. The LOD value obtained from this work (0.04 – 0.67  $\mu\text{gL}^{-1}$ ) was found to be comparable with the SPE technique using the most precise LC/MS detection [30], and was even lower than MSPE technique using similar LC/UV detector [11]. In addition, this method required a lower extraction time (14 min) compared to the membrane assisted micro-solid phase extraction (MA- $\mu$ -SPE) technique [31] with a silica-based sorbent. Therefore, the developed Ch-TEOS-DSPE-HPLC/UV extraction method with the aid of Box Behnken design optimization has excellent potential for analysing non-steroidal anti-inflammatory drugs in aqueous samples.

### CONCLUSION

The Box Benkhen design was successfully utilized with Ch-TEOS-DSPE-HPLC/UV to determine the maximum extraction efficiency of three selected non-steroidal anti-inflammatory drugs in water samples. The most significant parameters involved were sample pH > extraction time > desorption time. Optimum conditions were successfully applied to extract

naproxen, diclofenac and mefenamic acid from tap water and lake water. Good detection values at parts per billion levels (0.04-0.67  $\mu\text{gL}^{-1}$ ), good reproducibility and excellent recoveries (93.06 - 101.48%) were achieved using the proposed method. It can be concluded that the hybridizing high surface area nanoparticles of silica and biodegradable chitosan with high-loading functional groups increased the sorbent's surface properties and active sites. Thus, the proposed method presents several advantages such as simplicity, minimal use of sorbent, ease of operation, and low consumption of solvent, and thus can be a valuable tool to determine NSAIDs in aqueous matrices.

### ACKNOWLEDGEMENT

The authors would like to acknowledge funding from the Malaysian Ministry of Education through the Fundamental Research Grant Scheme (FRGS) with grant number: 600-IRMI/FRGS 5/3 (416/2019).

The authors declare that they have no conflict of interest.

### REFERENCES

1. Alvarez-Lorenzo, C., Blanco-Fernandez, B., Puga, A. M. and Concheiro, A. (2013) Crosslinked ionic polysaccharides for stimuli-sensitive drug delivery. *Adv. Drug Delivery Rev.*, **65**, 1148–1171.
2. Razavi, N. and Yazdi, A. S. (2017) New application of chitosan-grafted polyaniline in dispersive solid-phase extraction for the separation and determination of phthalate esters in milk using high-performance liquid chromatography. *J. Sep. Sci.*, **40(8)**, 1739–1746.
3. Park, D., Yun, Y. -S. and Park, J. M. (2010) The past, present, and future trends of biosorption. *Biotechnol. Bioprocess Eng.*, **15**, 86–102.

- 141 Nor Suhaila Mohamad Hanapi, Nur Husna Zainal Abidin, Wan Nazihah Wan Ibrahim, Nordiana Suhada Mohamad Tahiruddin, Nurul Auni Zainal Abidin, Roswanira Abdul Wahab and Sheela Chandren
- Bio-Nanohybrid Composite Sorbent-Based Microextraction Combined with High-Performance Liquid Chromatography for NSAIDs in Aqueous Samples
4. Chen, X., Lam, K. F., Mak, S. F. and Yeung, K. L. (2011) Precious metal recovery by selective adsorption using biosorbents. *J. Hazard. Mater.*, **186**, 902–910.
5. Sharififard, H., Ashtiani, F. Z. and Soleimani, M. (2013) Adsorption of palladium and platinum from aqueous solutions by chitosan and activated carbon coated with chitosan. *Asia-Pac. J. Chem. Eng.*, **8**, 384–395.
6. Du, H., Liu, M., Yang, X. and Zhai, G. (2015) The design of pH-sensitive chitosan-based formulations for gastrointestinal delivery. *Drug Discov.*, **20(8)**, 1004–1011.
7. Diagboya, P. N. E. and Dikio, E. D. (2018) Silica-based mesoporous materials; emerging designer adsorbents for aqueous pollutants removal and water treatment. *Micro. Meso. Mater.*, **266**, 252–267.
8. Soltani, R. D. C., Khataee, A. R., Safari, M. and Joo, S. W. (2013) Preparation of biosilica/chitosan nanocomposite for adsorption of a textile dye in aqueous solutions, *Int. Biodeter. Biodegr.*, **85**, 383–391.
9. Escobar, C. C., Dartora, M. H., Campo, L. F., Radtke, C., Bayne, J. M., Butler, I. S., Lattuada, R. M. and Santos, J. H. Z. (2014) The role of the sol-gel route on the interaction between rhodamine B and A silica matrix. *J. Sol-Gel Sci. Technol.*, **72**, 260–272.
10. Al-Sagheer, F. and Muslim, S. (2010) Thermal and Mechanical Properties of Chitosan/SiO<sub>2</sub> Hybrid Composites. *J. Nanomaterial*, Article ID 490679, 7 pages.
11. Marsin, F. M., Ibrahim, W. A. W., Keyo, A. S. A. and Sanagi, M. M. (2018) Box-behnken experimental design for the synthesis of magnetite-polypyrrole composite for the magnetic solid phase extraction of nonsteroidal anti-inflammatory drug residues. *Anal. Letter*, **51(14)**, 2221–2239.
12. Hanapi, N. S. M., Sanagi, M. M., Ismail, A. K., Saim, N., Ibrahim, W. N. W., Ibrahim, W. A. W. and Marsin, F. M. (2018) Rapid determination of non-steroidal anti-inflammatory drugs in aquatic matrices by two phase micro-electrodriven membrane extraction combined with liquid chromatography. *J. Chromatogr. Sci.*, **56(2)**, 166–176.
13. Budnyak, T. M., Pylypchuk, I. V., Tertykh, V. A., Yanovska, E. S. and Kolodynska, D. (2015) Synthesis and adsorption properties of chitosan-silica nanocomposite prepared by sol-gel method. *Nanoscale Res. Letters*, **10(87)**.
14. Ibrahim, W. N. W., Sanagi, M. M., Hanapi, N. S. M., Kamaruzaman, S., Yahaya, N. and Ibrahim, W. A. W. (2018) Solid-phase microextraction based on an agarose-chitosan-multiwalled carbon nanotube composite film combined with HPLC–UV for the determination of non-steroidal anti-inflammatory drugs in aqueous samples. *J. Sep. Sci.*, **41**, 2942–2951.
15. Zhou, L. -C., Meng, X. -G., Fu, J. -W., Yang, Y. -C., Yang, P. and Mi, C. (2014) Highly efficient adsorption of chlorophenols onto chemically modified chitosan, *App. Surf. Sci.*, **292**, 735–741.
16. Li, F., Du, P., Chen, W. and Zhang S. (2007) Preparation of silica-supported porous sorbent for heavy metal ions removal in wastewater treatment by organic-inorganic hybridization combined with sucrose and polyethylene glycol imprinting. *Anal. Chim. Acta*, **585**, 211–218.
17. Venkatesan, J., Jayakumar, R., Mohandas, A., Bhatnagar, I., and Kim, S. K. (2014) Antimicrobial activity of chitosan-carbon nanotube hydrogels. *Materials*, **7**, 3946–3955.
18. Coradin, T., Allouche, J., Boissiere, M. and Livage, J. (2006) Sol-gel biopolymer/silica nanocomposites in biotechnology. *Curr. Nanosci.*, **2(3)**, 219–230.
19. Hemsri, S., Asandei, A. D., Grieco, K. and Parnas, R. S. (2011) Biopolymer composites of wheat gluten with silica and alumina. *Composites: Part A*, **42**, 1764–1773.
20. Zhang, S., Xu, F., Wang, F., Zhang, W., Peng, X. and Pepe, F. (2013) Silica modified calcium alginate-xanthan gum hybrid bead composites for the removal and recovery of Pb(II) from aqueous solution. *Chem. Eng. J.*, **234**, 33–42.
21. Ibrahim, W. N. W., Sanagi, M. M., Hanapi, N. S. M., Kamaruzaman, S., Yahaya, N. and Ibrahim, W. A. W. (2018) Solid-phase microextraction based on an agarose-chitosan-multiwalled carbon nanotube composite film combined with HPLC–UV for the determination of nonsteroidal anti-inflammatory drugs in aqueous samples. *J. Sep. Sci.*, **41(14)**, 2942–2951.
22. Ibrahim, W. N. W., Sanagi, M. M., Hanapi, N. S. M., Hadzir, N. M., Yahaya, N. and Kamaruzaman, S. (2020) Agarose-chitosan-intergrated multi-walled carbon nanotubes film solid phase microextraction combined with high performance liquid chromatography for the determination of tricyclic antidepressant drugs in aqueous samples. *Malaysian J. Anal. Sci.*, **24(1)**, 33–41.

- 142 Nor Suhaila Mohamad Hanapi, Nur Husna Zainal Abidin, Wan Nazihah Wan Ibrahim, Nordiana Suhada Mohamad Tahiruddin, Nurul Auni Zainal Abidin, Roswanira Abdul Wahab and Sheela Chandren
- Bio-Nanohybrid Composite Sorbent-Based Microextraction Combined with High-Performance Liquid Chromatography for NSAIDs in Aqueous Samples
23. Saad, S. M., Aling, N. A., Miskam, M., Saaid, M., Zain, N. N. M., Kamaruzaman, S., Raoov, M., Hanapi, N. S. M., Ibrahim, W. N. W. and Yahaya, N. (2020) Magnetic nanoparticles assisted dispersive liquid–liquid microextraction of chloramphenicol in water samples. *Royal Society Open Sci.*, **7**, **200143**, E-ISSN 2054–5073.
24. Othman, N. Z., Hanapi, N. S. M., Ibrahim, W. N. W. and Saleh, S. H. (2020) Alginate incorporated multi-walled carbon nanotubes as dispersive micro solid phase extraction sorbent for selective and efficient separation of acidic drugs in water samples. *Nature Environ. Poll. Technol.*, **19**(3), 155–1162.
25. Zheng, M., Wang, S., Hu, W. and Feng, Y. (2010) In-tube solid-phase microextraction based on hybrid silica monolith coupled to liquid chromatography-mass spectrometry for automated analysis of ten antidepressants in human urine and plasma. *J. Chromatogr. A*, **1217**, 74937501.
26. Song, X. Y., Shi, Y. P. and Chen, J. A. (2012) Novel extraction technique based on carbon nanotubes reinforced hollow fiber solid/liquid microextraction for the measurement of piroxicam and diclofenac combined with high performance liquid chromatography. *Talanta*, **100**, 153–161.
27. Joglekar, A. M. and May, A. T. (1987) Product excellence through design of experiments. *Cereal Foods World*, **32**, 857–868.
28. Safraz-Yazdi, A., Fatehyan, E. and Amiri, A. (2014) Determination of mercury in real water samples using in situ derivatization followed by sol-gel–solid-phase microextraction with gas chromatography–flame ionization detection. *J. Chromatogr. Sci.*, **52**, 81–87.
29. Sousa, C. T., Nunes, C., Proenc, M. P., Leitao, D. C., Lima, J. L. F. C., Reis, S., Araujo, J. P. and Lucio, M. (2012) pH sensitive silica nanotubes as rationally designed vehicles for nsaid delivery. *Colloid Surface B*, **94**, 288–295.
30. Dahane, S., Galera, M. M., Marchionni, M. E., Sodal Viciano, M. M., Derdour, A. and Gil Gartia, M. D. (2016) Mesoporous Silica Based MCM-41 as Solid-Phase Extraction Sorbent Combined with Micro-Liquid Chromatography-Quadrupole-Mass Spectrometry for the Analysis of Pharmaceuticals in Waters. *Talanta*, **152**, 378–391.
31. Lim, T. H., Hu, L., Yang, C., He, C. and Lee, H. K. (2013) Membrane Assisted Micro-Solid Phase Extraction of Pharmaceuticals with Amino and Urea-Grafted Silica Gel. *J. Chromatogr. A*, **1316**, 8–14.